Cell Metabolism, Volume *27*

Supplemental Information

CD38-NAD$^+$Axis Regulates Immunotherapeutic Anti-Tumor T Cell Response

Shilpak Chatterjee, Anusara Daenthanasanmak, Paramita Chakraborty, Megan W. Wyatt, Payal Dhar, Shanmugam Panneer Selvam, Jianing Fu, Jinyu Zhang, Hung Nguyen, Inhong Kang, Kyle Toth, Mazen Al-Homrani, Mahvash Husain, Gyda Beeson, Lauren Ball, Kristi Helke, Shahid Husain, Elizabeth Garrett-Mayer, Gary Hardiman, Meenal Mehrotra, Michael I. Nishimura, Craig C. Beeson, Melanie Gubbels Bupp, Jennifer Wu, Besim Ogretmen, Chrystal M. Paulos, Jeffery Rathmell, Xue-Zhong Yu, and Shikhar Mehrotra

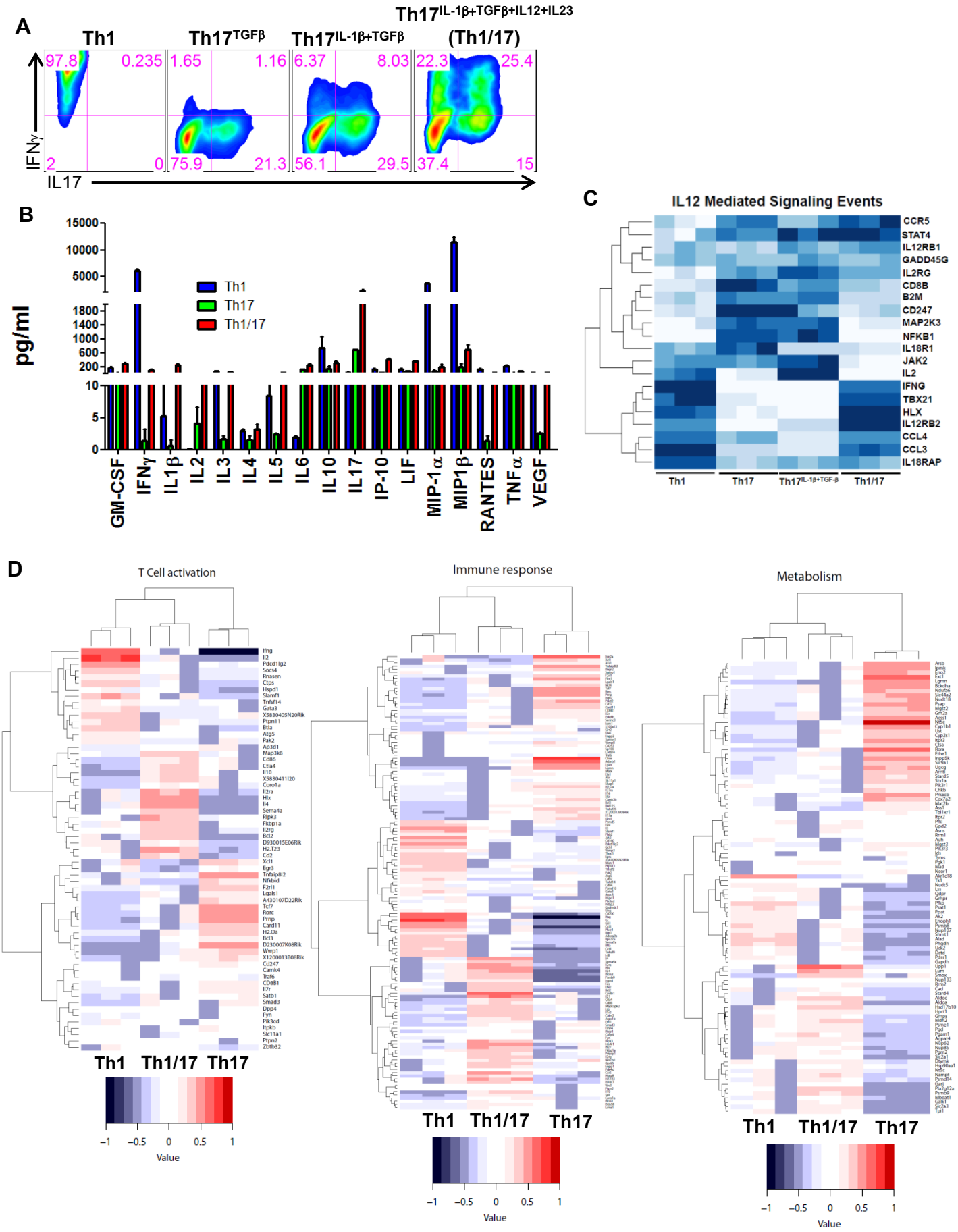

Figure S1. Related to Figure 1

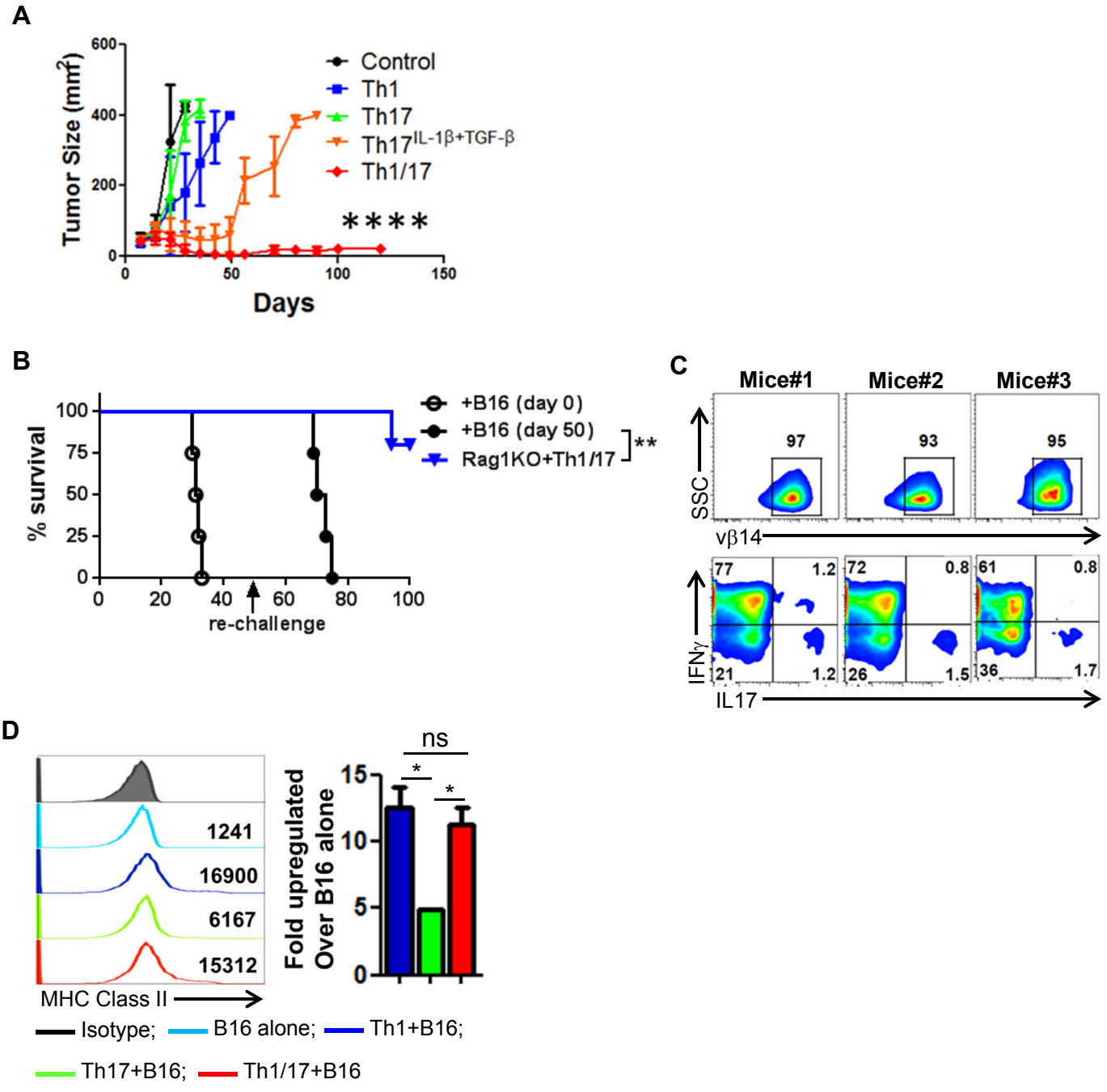

Figure S2. Related to Figure 2

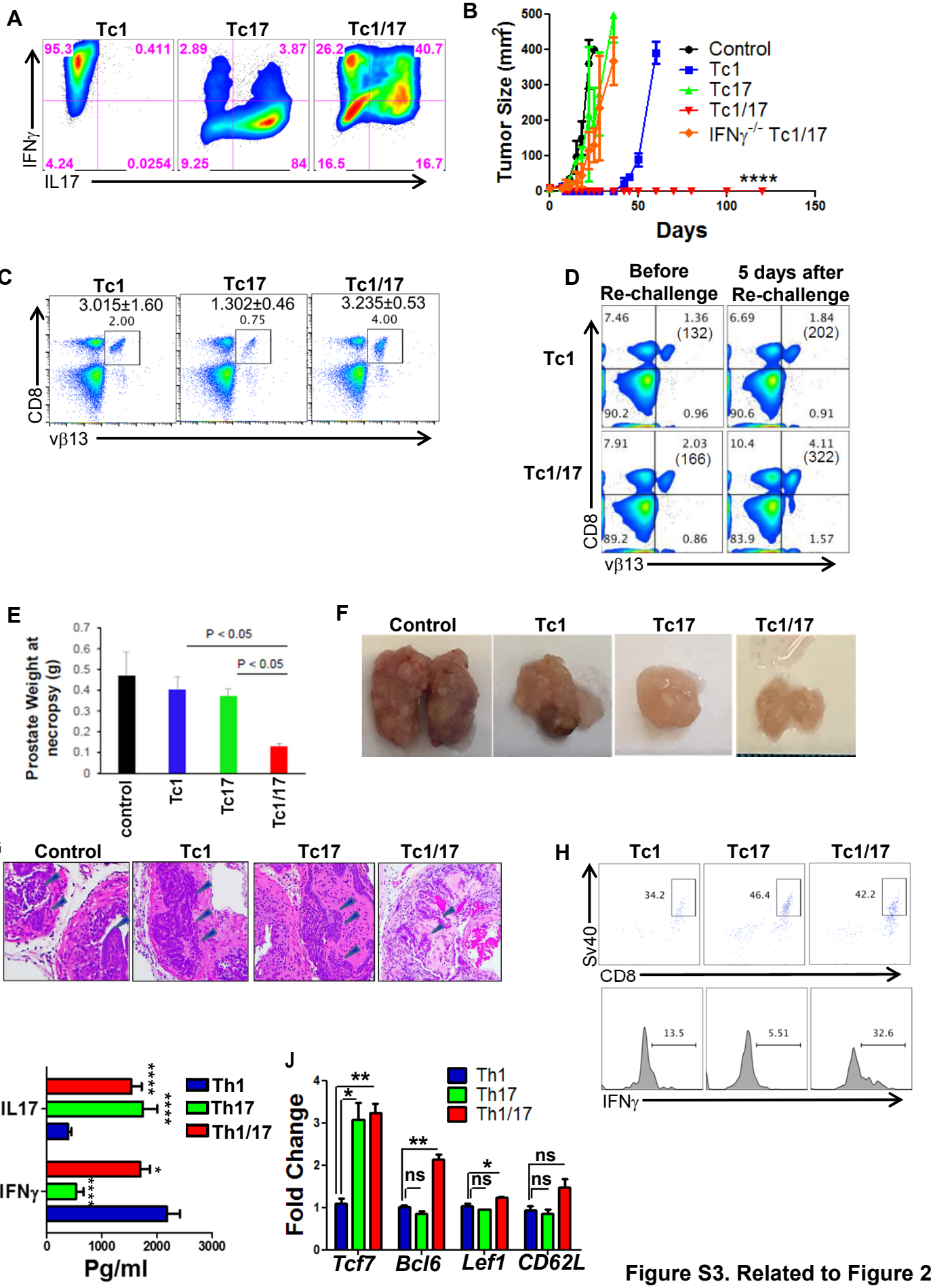

Figure S3. Related to Figure 2

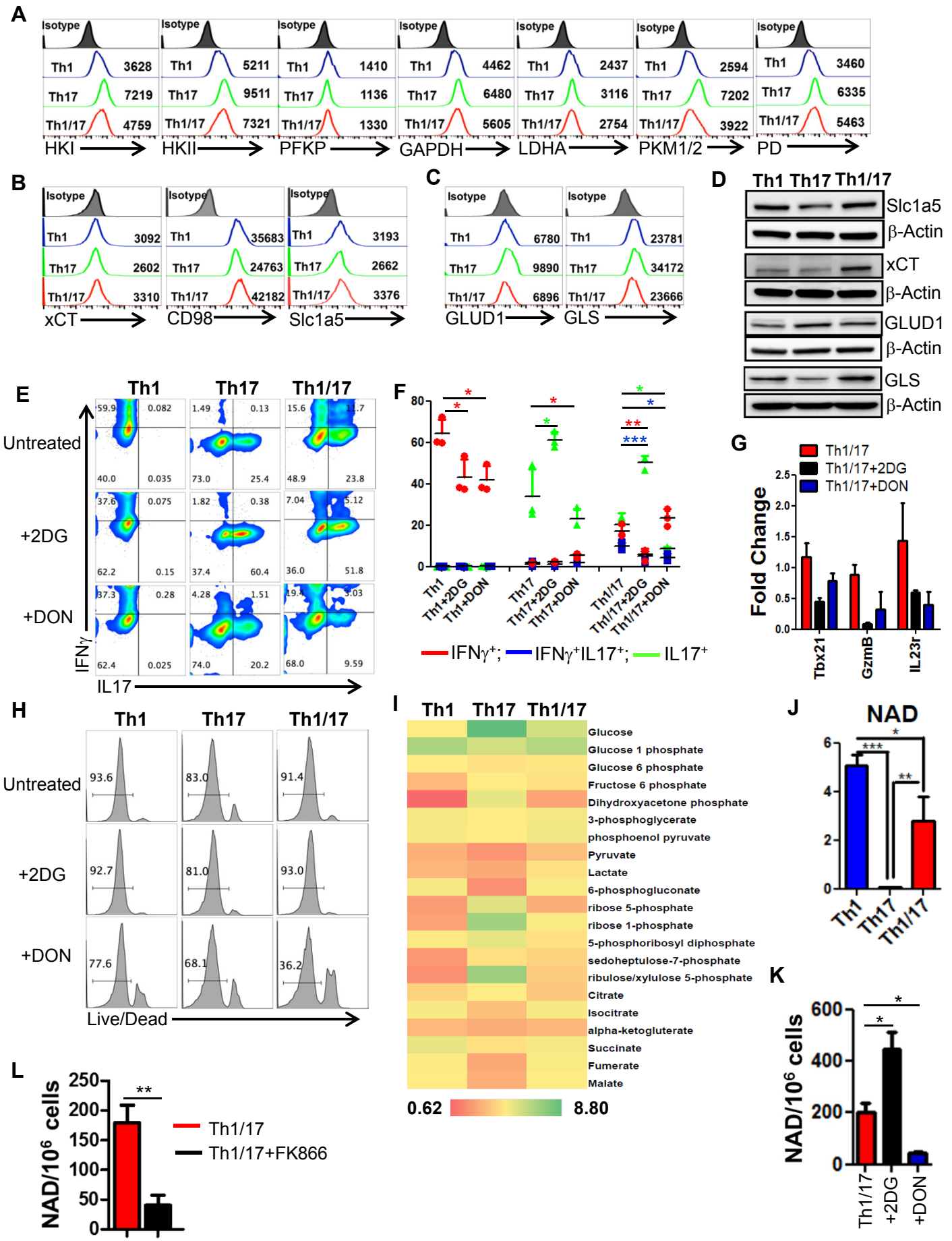

Figure S4. Related to Figure 3 & 4

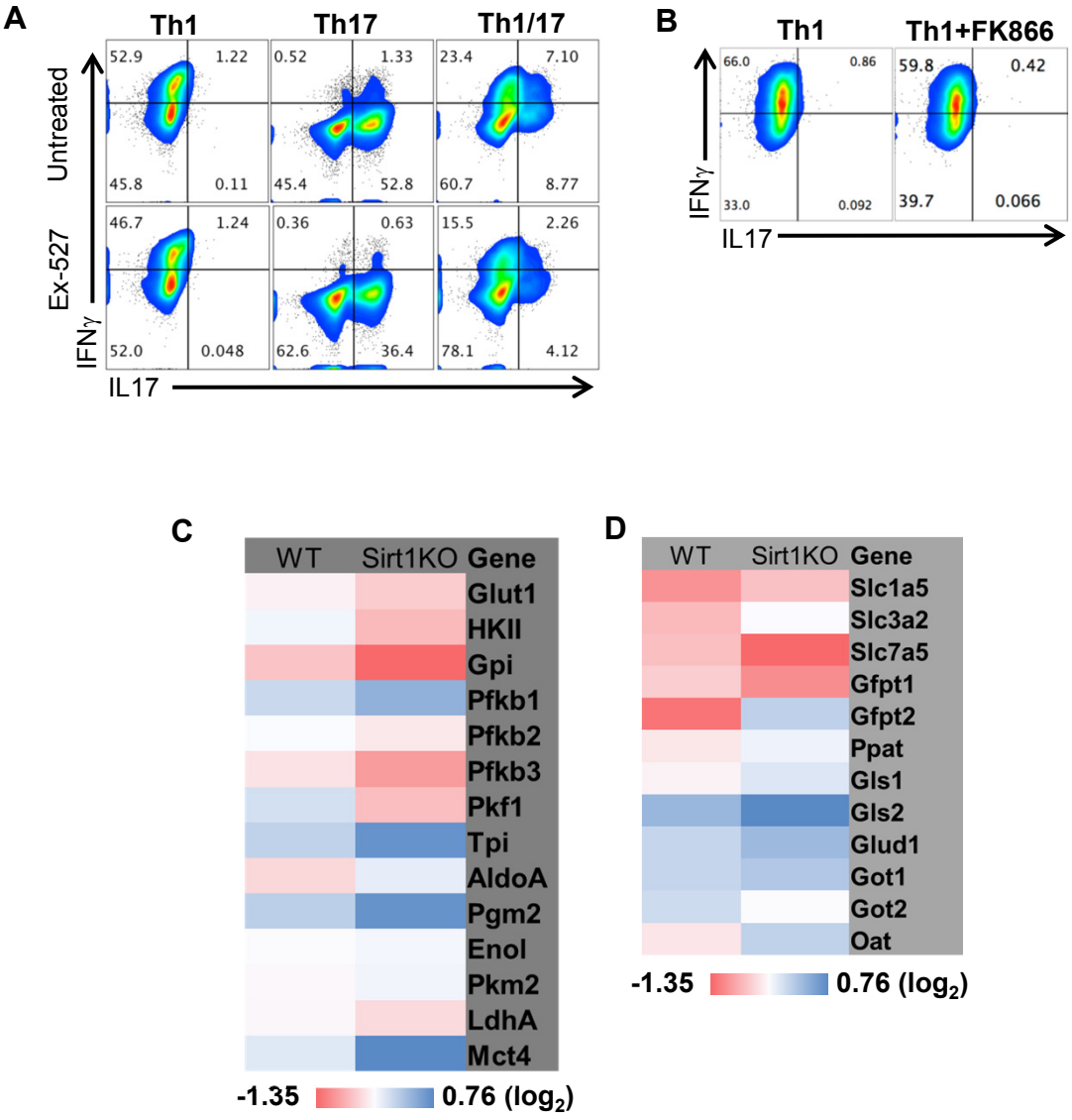

Figure S5. Related to Figure 5

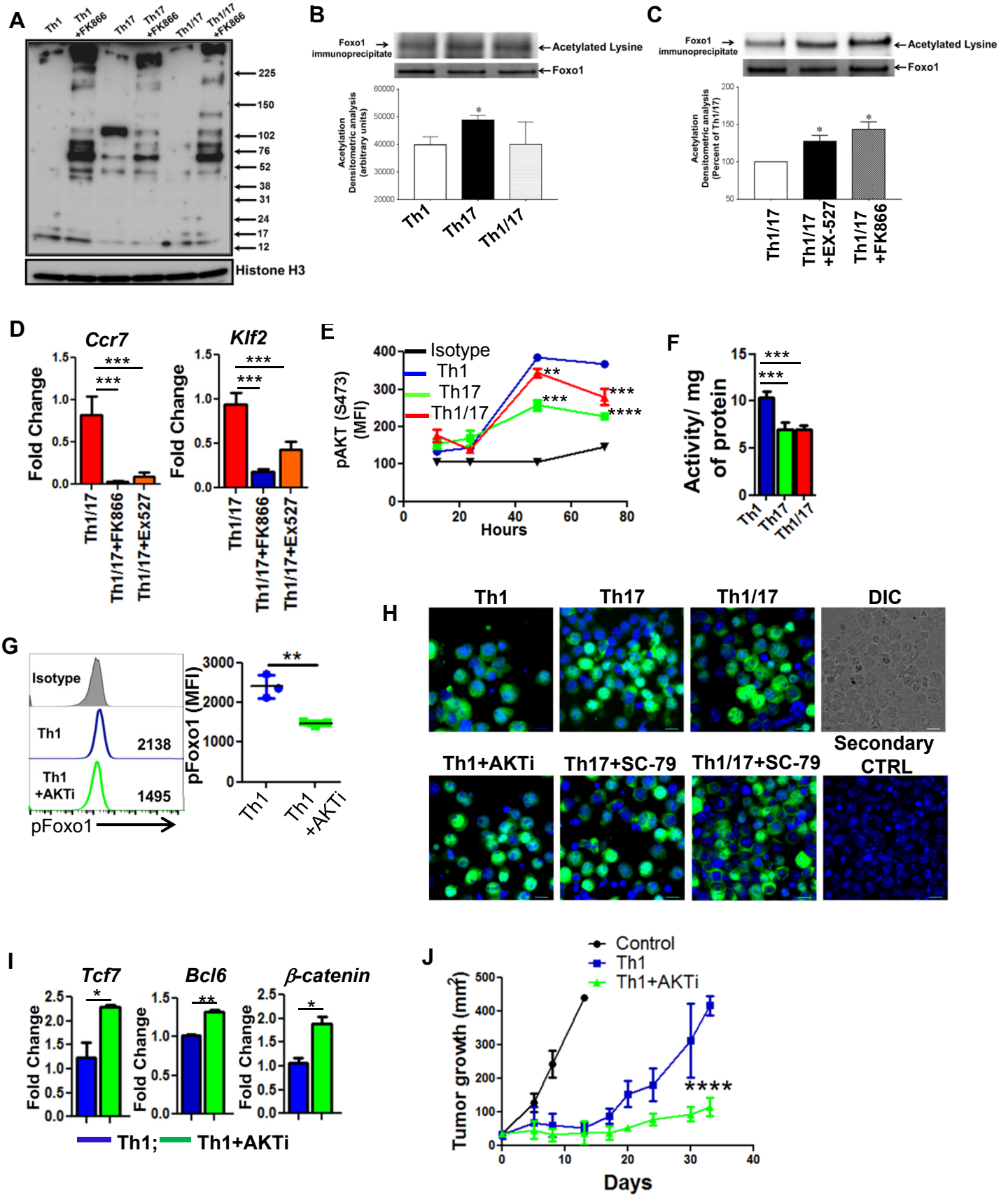

Figure S6. Related to Figure 6

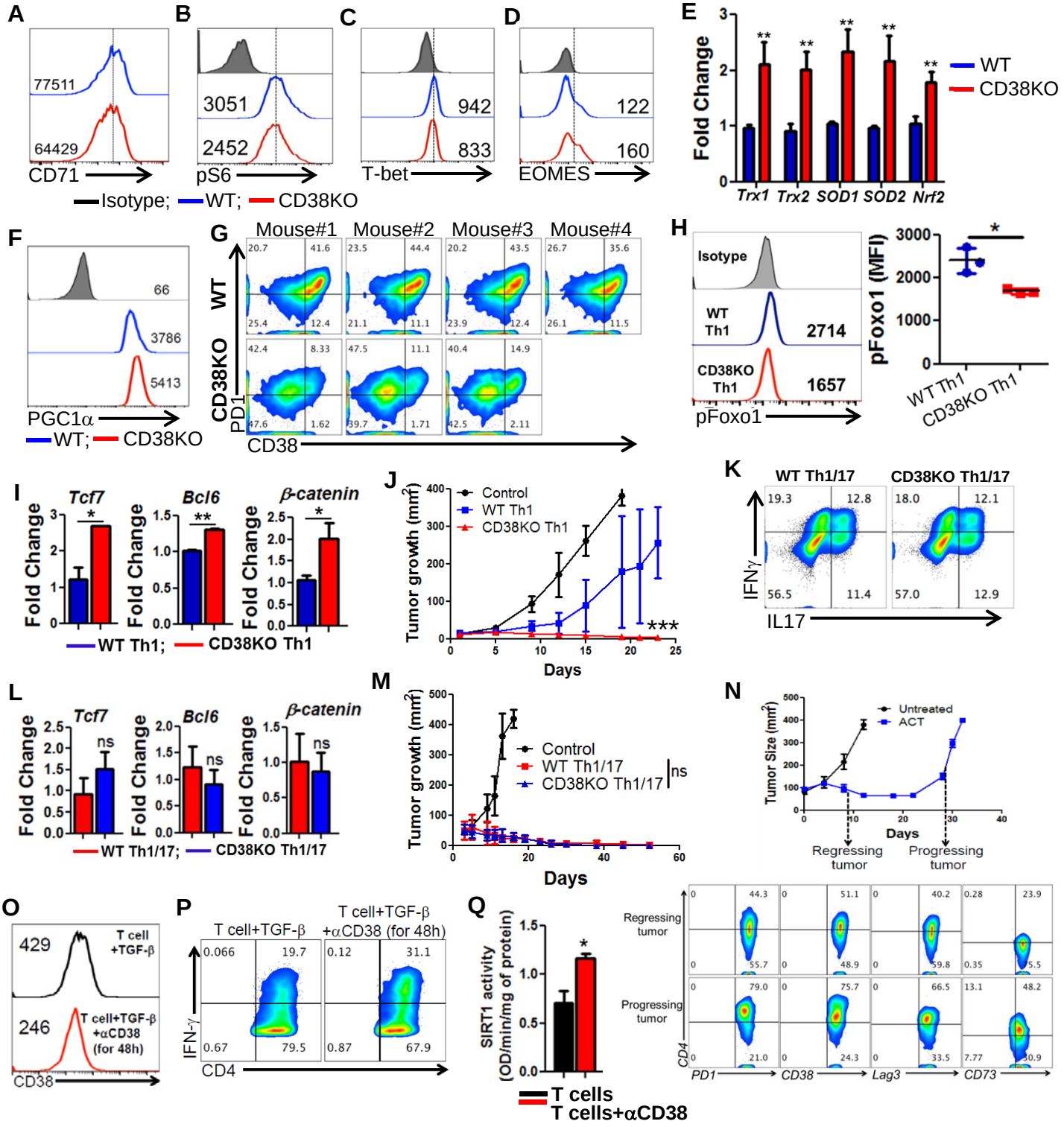

Figure S7. Related to Figure 7

Supplemental Figure legends

Figure S1. Related to Figure 1. Hybrid Th1/17 cells possess traits of both Th1 and Th17 cells.

A) Purified $CD4^+$ T cells differentiated *ex vivo* to Th1, Th17 and Th1/17 cells were re-stimulated for 4hr with PMA and ionomycin before the samples were stained with fluorochrome conjugated antibodies and acquired using flow cytometry. Data are representative of three independent experiments with similar results.

B) Purified $CD4^+$ T cells differentiated *ex vivo* to Th1, Th17 and Th1/17 cells were re-stimulated overnight with anti-CD3 (2μg/ml) + anti-CD28 (2μg/ml). Supernatant obtained after re-stimulation were evaluated for different cytokines and chemokines using multiplex assay.

C-D) Transcripts (obtained from Illumina bead array analysis) significant at <0.1 from Th1, Th17 and Th1/17 were compared using *Venny*, a tool for generating and visualizing area proportional Venn diagrams and 607 transcripts were common to both the Th1 vs Th1/17 and Th17 vs Th1/17 comparisons. Heatmap (*C* and *D*) represent the genes that mapped to T cell activation, immune response and metabolism pathways.

Figure S2. Related to Figure 2. Hybrid Th1/17 cells exhibit superior anti-tumor response.

A) HLA-$A2^+$ (n=8 mice/group) mice were inoculated (*s.c.*) with 0.25×10^6 B16-F10-HLA-$A2^+$ murine melanoma cells and after nine days mice were either left as untreated control or treated by adoptively transferring 0.3×10^6 tyrosinase reactive TIL1383I TCR transgenic T cells differentiated to Th1, Th17, $Th17^{IL1\beta+TGF\beta}$ and hybrid Th1/17 cells. Tumor growth was measured using digital caliper every fourth day. Data in the figure demonstrates mean tumor size at each time point in one of the three experiments with similar results.

B-C) Rag1 deficient (Rag1KO) mice were *i.v.* injected with $0.5x10^6$ luciferase-transduced B16-F10. Lympho-depletion was induced one day prior to hybrid Th1/17 T cell transfer. B16-Fluc was infused for tumor re-challenge on day 50. *B)* Survival and tumor growth were followed. *C)* Representative flow panel depicts TILs recovered from lungs of Rag1KO mice on day 120 and analyzed for expression of

$V\beta14^{+}CD4^{+}$ T cells. Recovered TILs were stimulated with PMA and ionomycin before analysis for intracellular IFNγ and IL17 levels was done using flow cytometry. *D*) Flow cytometry analysis of MHC Class II expression on B16 melanoma cells was performed after overnight co-culture at 1:1 ratio with either *in vitro* differentiated TRP-1 Th1, Th17 or Th1/17 cells. Adjacent bar diagram represents fold upregulation of MHC class II expression on B16 melanoma from Th subset co-culture group over B16 alone. Data are representative of 3 independent experiments with similar results. **p*<0.05 and *****p*<0.0001

Figure S3. Related to Figure 2. Hybrid Tc1/17 cells is superior to Tc1 and Tc17 cells in controlling tumor.

A) Melanoma epitope gp100 reactive T cells obtained from Pmel TCR transgenic mouse were used for differentiation to Tc1, Tc17 and Tc1/17 cells using the similar protocol that was used to differentiate Th1/17 cells. These Tc subsets were then re-stimulated with PMA and ionomycin for 4h and analyzed for the intracellular cytokine accumulation using flow-cytometry. Data are representative of three independent experiments with similar results.

B-D) C57BL/6 mice (n=5 mice/group) were inoculated (*s.c.*) with 0.25×10^{6} B16-F10 murine melanoma cells and after nine days mice either left as untreated control or treated by adoptively transferring *ex vivo* differentiated 1×10^{6} Pmel Tc1, Th17, Tc1/17 or $IFN\gamma^{-/-}$ Tc1/17 cells. Tumor growth was measured using digital calipers every fourth day. *B)* Data in figure demonstrate mean tumor size at each time point. *C)* Persistence of adoptively transferred cells in the peripheral blood of tumor bearing mice following 21 days after ACT. *D)* The mice from the group which received Tc1 and Tc1/17 were re-challenged with B16-F10 tumors on day 50, and the transferred gp100 specific $V\beta13^{+}$ cells were tracked five days later in the blood using FACS.

E-H) TRAMP (Transgenic Adenocarcinoma of the Mouse Prostate) mice were adoptively transferred with either Sv40 antigen specific Tc1 or Tc17 or Tc1/17 cells and were euthanized 57 days post ACT for detailed analysis. *E*) Graph depicts the prostate weight of mice at necropsy showing significant reduction in prostate weight of TRAMP mice that were treated by adoptively transferred Tc1/Tc17 cells, as

compared to those treated with either Tc1 or Tc17 cells alone. *F*) Representative images of the prostate from TRAMP mice treated in *E* are shown. *G*) Representative micrographs of H&E staining showing the histology of the prostate from TRAMP mice. Arrowheads indicate tumors in the prostate gland. *H*) Flow cytometry analyses demonstrating significantly higher IFNγ secretion (*lower panel*) within the Sv40 tetramer specific $CD8^+$ T cells (*upper panel*). *I*) Peripheral blood from normal healthy human donor was used to purify $CD4^+$ T cells using magnetic beads and subjected to differentiation *ex vivo* to Th1, Th17 and Th1/17 cells. These Th subsets were re-stimulated overnight with anti-CD3 (2 μg/ml) and anti-CD28 (2 μg/ml) and the supernatant collected was characterized for IFNγ and IL17 levels using ELISA. *J*) RNA prepared from human Th1, Th17 and Th1/17 cells was used for qPCR based analysis of various stemness associated genes. *p<0.05, **p< 0.01 and ***p<0.005, ****p<0.0001

Figure S4. Related to Figure 3 and 4. Metabolic commitment of Th1, Th17 and Th1/17 cells.

A-C) *In vitro* differentiated murine Th1, Th17 and Th1/17 cells were used for determining: *A*) intracellular expression of various glycolytic enzymes, *B*) cell surface expression of different amino acid transporters, and *C*) intracellular expression of glutaminolytic enzymes by flow cytometry. Data are representative of three independent experiments with similar results. *D*) Western blot analysis determined the protein level of various glutamine transporters and glutaminolytic enzymes in *in vitro* differentiated Th1, Th17 and Th1/17 cells. β-actin was used as a loading control. Data are representative of two independent experiments with similar results.

E-F) Purified $CD4^+$ T cells were differentiated to Th1, Th17 and Th1/17 cells either in presence or absence of 2DG (1mM) or DON (3μM) and characterized for: *E*) intracellular cytokine secretion after re-stimulating them with PMA and ionomycin for 4hr, *F*) determining the frequency of cells that were $IFN\gamma^+$, $IL17^+$ or $IFN\gamma^+IL17^+$ in each treatment groups and presented using scatter plot. Statistical comparison between treated and untreated groups are indicated with red asterisk for $IFN\gamma^+$, green asterisk for $IL17^+$, and blue asterisk for $IFN\gamma^+IL17^+$ cells. *G*) RNA preparation that was used for qPCR based analysis of various effector genes, and *H*) determining the percentage of viable cells by FACS based staining with live/dead dye. Numerical values represent the percent gated viable cells. Data are representative of three independent experiments with identical results.

I) Purified $CD4^+$ T cells were differentiated into Th1, Th17 and Th1/17 cells and intracellular metabolites were measured using mass spectrometry. Depicted heat maps are the representation of the relative amount of each metabolite from Glycolysis, PPP and TCA cycle.

J) Th1, Th17 and Th1/17 cells were used for determining intracellular levels of NAD^+.

K and L) Th1/17 cells differentiated *ex vivo* either in presence of vehicle control or *K)* 2DG (1mM) or DON (3μM), *L)* or FK866 (10nM) were used to determine intracellular levels of NAD^+. Data are representative of three independent experiments with similar results.

**p*<0.05, ***p*< 0.01 and ****p*<0.005.

Figure S5. Related to Figure 5. Loss of Sirt1 expression and NAD^+ levels on Th1/17 cell phenotype and function.

A) Purified $CD4^+$ T cells from C57BL/6 were used to differentiate to Th1/17 cells either alone or in the presence of Ex527, a pharmacological inhibitor of Sirt1. Cells were then restimulated with PMA and ionomycin for 4hr in presence of golgi block to stain for intracellular accumulation of cytokines IFNγ and IL17. *B*) Th1 cells were cultured either in presence or absence of NAD^+ inhibitor FK866 (10nM) and intracellular staining was performed for IFNγ and IL17. Data was acquired using FACS and analysis was carried out using FlowJo software.

C-D) Purified splenic $CD4^+$ T cells from either C57BL/6 WT or $Sirt1^{fl/fl}CD4^{Cre}$ (Sirt1KO) mouse were used to *ex vivo* program for Th1/17 cells. RNA was prepared and quantitative PCR analysis was performed for the expression of various glycolysis (*C*) and glutaminolysis (*D*) associated genes in either WT or Sirt1KO Th1/17 cells. Data in section *A-D* are representative of three independent experiments.

Figure S6. Related to Figure 6. Acetylation levels of Foxo1 regulate Th1/17 phenotype and function.

A) Purified $CD4^+$ T cells differentiated to Th1, Th17 and Th1/17 (with or without NAD^+ inhibitor FK866) were used for determining global acetylation of nuclear protein using western blot, where membrane was

probed with anti-acetylated lysine antibody followed by incubation with peroxidase conjugated secondary antibody. Membrane was blotted for Histone H3 (bottom panel) for loading correction.

B-C) Foxo1 was immuneprecipitated from either (*B*) Th1, Th17 and Th1/17 cells or (*C*) Th1/17 cells treated with either Ex527 (10μM) or FK866 (10nM), using anti-Foxo1 monoclonal antibody for 16h at 4°C followed by incubation with Protein A/G-Sepharose for 1h at 4°C. The immunoprecipitated Foxo1 was separated on 10% SDS-PAGE and then transferred to nitrocellulose membranes. The membranes were probed with anti-Acetyl-Lysine antibody (1:1000 dilution) followed by incubation with secondary antibody (HRP-conjugated goat anti-rabbit IgG at 1:3000 dilution) for 1h at 20°C as previously described. For chemiluminescent detection, the membranes were treated with enhanced chemiluminescent reagent (ECL), and the signal was monitored using a Biorad Versadoc imaging system (Biorad, Hercules, CA). Total Foxo levels in the samples are shown below the immunoprecipitation blot. Bars represent quantified differences in Foxo acetylation between samples. Data represent mean ± SE; *$p < 0.05$; n = 3.

D) qPCR analysis for the expression of *Klf2* and *Ccr7* in Th1/17 cells differentiated either in presence or absence of FK866 (10nM) or Ex527 (10μM) was performed.

E) AKT phosphorylation (at S473) was determined in Th1, Th17 and Th1/17 cells using flow-cytometery. Mean fluorescence intensity (MFI) of pAKT (S473) at different time point is depicted, and statistical analysis determining the significance of reduction as compared to Th1 group is shown. **p< 0.01 and ***p<0.005, ****p<0.001. *F)* Purified $CD4^+$ T cells differentiated to Th1, Th17 and Th1/17 cells were used to determine the kinase activity of AKT using an ELISA based method flowing the manufacturer's protocol. Data are representative of 3 independent experiments with identical observation. *G*) Purified $CD4^+$ T cells were differentiated to Th1 cells either in the presence or absence of AKT inhibitor (AKTi; 1μM) and used for determining phosphorylation of Foxo1 (S257) by flow cytometry. Overlay plot with numerical values representing mean fluorescence intensity (MFI) from one representative experiment is shown. Cumulative data from three independent experiments with similar result is shown on right. (*H*) As in *G)*, $CD4^+$ T cells were differentiated to Th17 and Th1/17 in the absence or presence of AKT activator SC-79 (0.5 μg/ml) before confocal imaging was performed to determine the localization of Foxo (green). Nuclei were stained with DAPI (blue). Bar represents 10 μM.

(I) Cells in *G)* were used to determine the expression of various stemness associated genes using qPCR, and (*J*) ability to control growth of *s.c.* established B16-F10-HLA-A2^{+} murine melanoma upon adoptive transfer. Tumor growth was measured using digital calipers every fourth day. Data in figure demonstrate mean tumor size at each time point in one of the two experiments with similar results. *p<0.05, **p< 0.01 and ***p<0.005.

Figure S7. Related to Figure 7. Inverse correlation between CD38 and NAD^{+} regulates anti-tumor property of T cells.

(*A*-*F*) Splenic T cells from WT or CD38KO were used for TCR mediated activation using anti-CD3 and anti-CD28 for three days in presence of rIL2 (50 units/ml). Activated cells were then used for various assays. Flow cytometry based analysis for the cell surface expression of (*A*) CD71, (*B*) intracellular expression of pS6, (*C*) T-bet and (*D*) EOMES. (*E*) qPCR analysis of the expression of various anti-oxidant genes, and (*F*) flow cytometry analysis of the intracellular expression of PGC1α. Numerical values in *A*-*D* and *F* are mean fluorescence intensity. *G*) CD4^{+} T cells from either WT or CD38KO IFNγ$^{Thy1.1}$ knock in mice were retrovirally transduced with TIL1383I TCR and adoptively transferred (0.5×10^{6} cells/mouse) to HLA-A2^{+} mice with ten days subcutaneously established B16-F10-HLA-A2^{+} melanoma tumors. TILs were retrieved and expression of PD1 *vs.* CD38 was evaluated on transferred CD4^{+} Vβ12^{+} TIL1383I TCR specific cells using flow cytometry.

H-*J*) Purified CD4^{+} T cells from either WT or CD38KO mice differentiated to Th1 cells were used for determining: (*H*) phosphorylation of Foxo1 (S257) by flow cytometry. Scatter plot representing cumulative data for mean fluorescence intensity (MFI) from three independent experiments. (*I*) qPCR analysis of various stemness associated genes was performed on samples used in parallel experiments in *H*. *J)* ability to control the growth of 10 days subcutaneously established B16-F10 melanoma tumor in C57BL/6 mice (n=4 mice/group) upon adoptive transfer of either WT or CD38KO TRP-1 TCR transduced Th1 cells (0.5×10^{6} cells/mouse). Tumor growth curve averaged from different mice in various experimental groups of recipient mice is shown.

K-L) Purified $CD4^+$ T cells from either WT or CD38KO mice differentiated to Th1/17 cells were used to determine: (*K*) intracellular cytokine secretion after re-stimulating them with PMA and ionomycin for 4hr; (*L*) qPCR based mRNA levels for key stemness associated genes; (*M*) ability to control the growth of 10 days subcutaneously established B16-F10 melanoma tumor in C57BL/6 mice (n=4mice/group) upon adoptive transfer of either WT or CD38KO TRP-1 TCR transduced Th1/17 cells (0.5×10^6 cells/mouse). Tumor growth curve averaged from different mice in various experimental groups of recipient mice is shown.

N) $CD4^+$ TRP-1 T cells were activated *in vitro* for 3 days and adoptively transferred (1×10^6 cells/mouse) in a group of 8 mice with subcutaneously established B16-F10 melanoma tumors. A group of 4 mice were euthanized either on day 8 or day 28 post ACT (upper panel) and TILs were retrieved from the tumor site to evaluate for the expression of various negative regulatory molecules within the $CD4^+$ $V\beta14^+$ gate using flow cytometry (lower panel).

O-Q) C57BL/6 (WT) derived splenic $CD4^+$ T cells were activated for three days in presence of TGF-β (1 ng/ml) and treated with or without of anti-CD38 (5 μg/ml) antibody for last 48h of culture. Activated cells from these groups were then used for flow cytometric analysis to determine the expression of CD38 (*O*), intracellular staining of IFNγ (*P*), and nuclear Sirt1 activity (*Q*).

R-T) WT T cells labelled with CFSE (1μM) were co-cultured at 1:1 ratio with either (*R*) MDSCs isolated from the tumor site of WT or CD38KO mouse, or (*S*) *in vitro* differentiated iTreg from WT or CD38KO for three days in presence of anti-CD3 (1μg/ml) and anti-CD28 (1μg/ml). T cells without anti-CD3 and anti-CD28 activation were kept as control. Suppression of T cell proliferation was determined by CFSE dilution using flow cytometry. Numerical values in *R* represent percent proliferating cells that correspond to each division.

T) Activated NK cells ($CD3^-NK1.1^+$) from either WT or CD38KO mice were stimulated for 5h with PMA and ionomycin on day four of the culture, and intracellular cytokine secretion was evaluated by flow cytometry. Numerical values represent percent IFNγ secreting cells.

Data presented in sections *A-E*, *H-I*, *J*, *K-L* and *N-T* are representative of three experiments, whereas data in section *F* is from one in four independent experiment with similar results. *p<0.05, **p< 0.01 and ***p<0.005.

Table S1: Related to Figure 3. *p* value for glycolytic genes expression in Th1, Th1 and Th1/17 cells

Gene name	Th1 *vs.* Th17	Th1*vs*. Th1/17	Th17 *vs.* Th1/17
Glucose transporter 1 (Glut1)	0.04013	0.00181	0.96403
Hexokinase 1 (HK1)	0.15463	0.01092	0.80529
Hexokinase 2 (HK2)	0.05468	0.00251	0.94528
Glucose-6-phosphate isomerase (Gpi)	0.08248	0.07438	0.91092
Phosphofructokinase b 1 (Pfkb1)	0.01116	0.01188	0.12497
Phosphofructokinase b 2 (Pfkb2)	0.22222	0.22473	0.88340
Phosphofructokinase b 3 (Pfkb3)	0.84016	0.78659	0.99723
Phosphofructokinase 1 (Pfk1)	0.00816	0.00261	0.17861
Triose Phosphate isomerase (Tpi)	0.01430	0.02120	0.10837
Aldolase A	0.04038	0.05181	0.80448
Phosphoglycerate mutase 1 (Pgam1)	0.04068	0.48843	0.00561
Phosphoglucomutase 2 (Pgm2)	0.09448	0.12308	0.05527
Enolase (Enol)	0.00278	0.00909	0.12473
Pyruvate kinase 2 (Pkm2)	0.03252	0.03600	0.01143
Lactate dehrodenase A (LdhA)	0.01342	0.00862	0.04871
Monocarboxylate transporter 4 (MCT4)	0.01342	0.00862	0.04871

Table S2: **Related to Figure 3. *p* value for glutaminolysis genes expression in Th1, Th1 and Th1/17 cells**

Gene name	Th1 *vs.* Th17	Th1*vs*. Th1/17	Th17 *vs.* Th1/17
Solute carrier family 1 member 5 (Slc1a5)	0.10571	0.01140	0.02497

Solute carrier family 3 member 2 (Slc3a2)	0.04713	0.03538	0.01239
Solute carrier family 7 member 5 (Slc7a5)	0.05303	0.01560	0.00765
Glutamine-fructose-6-phosphate transaminase 1 (Gfpt1)	0.00856	0.02245	0.00669
Glutamine-fructose-6-phosphate transaminase 2 (Gfpt2)	0.01416	0.15260	0.12616
Phosphoribosyl pyrophosphate Amidotransferase (Ppat)	0.01199	0.19293	0.01605
Glutaminase 1(Gls1)	0.35285	0.14691	0.09248
Glutaminase 2 (Gls2)	0.05839	0.09548	0.02848
Glutamate dehydrogenase 1 (Glud1)	0.90391	0.01053	0.01413
Glutamate oxaloacetate transaminase 1 (Got1)	0.04930	0.24485	0.02564
Glutamate oxaloacetate transaminase 2 (Got2)	0.17816	0.15652	0.00212
Ornithine aminotransferase (Oat)	0.04263	0.11451	0.02350

Table S3: Related to Figure 7. *p* value for glutaminolysis genes expression in WT and CD38KO CD4$^+$ T cells

Gene name	WT *vs.* CD38KO CD4$^+$ T cells
Solute carrier family 1 member 5 (Slc1a5)	0.113438
Solute carrier family 3 member 2 (Slc3a2)	0.045317
Solute carrier family 7 member 5 (Slc7a5)	0.021036
Glutamine-fructose-6-phosphate transaminase 1 (Gfpt1)	0.049051
Glutamine-fructose-6-phosphate transaminase 2 (Gfpt2)	0.057432
Phosphoribosyl pyrophosphate Amidotransferase (Ppat)	0.194268
Glutaminase 1(Gls1)	0.039745
Glutaminase 2 (Gls2)	0.043545

Glutamate dehydrogenase 1 (Glud1)	0.137267
Glutamate oxaloacetate transaminase 1 (Got1)	0.050179
Glutamate oxaloacetate transaminase 2 (Got2)	0.019091
Ornithine aminotransferase (Oat)	0.034764

Table S4: Related to STAR methods

Mouse qPCR primers: 5'-3'			
Gene	**Forward**	**Reverse**	**Source**
Glut1	CAGTTCGGCTATAACACTGGTG	GCCCCCGACAGAGAAGATG	IDT, Coralville
HKI	CGGAATGGGGAGCCTTTGG	GCCTTCCTTATCCGTTTCAATGG	IDT, Coralville
HKII	GGAACCGCCTAGAAATCTCC	GGAGCTCAACCAAAACCAAG	IDT, Coralville
Gpi	TCAAGCTGCGCGAACTTTTTG	GGTTCTTGGAGTAGTCCACCAG	IDT, Coralville
Pfkb1	ATGAGCTGCCCTATCTCAAGT	GTCCCGGTGTGTGTTCACAG	IDT, Coralville
Pfkb2	GACAAGCCAACTCACAACTTCC	ACACTGTAATTTCTTGGACGCC	IDT, Coralville
Pfkb3	CCCAGAGCCGGGTACAGAA	GAGCCCCACCATCACAATCAC	IDT, Coralville
Pfk	AGGAGGGCAAAGGAGTGTTT	TTGGCAGAAATCTTGGTTCC	IDT, Coralville
Tpi	CTTACATCGACTTTGCCAGACA	CTAGGGCGTGGCTCACTTT	IDT, Coralville
AldoA	TCAGTGCTGGGTATGGGTG	GCTCCTTAGTCCTTTCGCCT	IDT, Coralville
Pgam1	TCTGTGCAGAAGAGAGCAATCC	CTGTCAGACCGCCATAGTGT	IDT, Coralville
Pgm2	AGTGAAGACGCAGGCATATCC	GGCTCCACGGTAGAGACGA	IDT, Coralville

Enol	AAAGATCTCTCTGGCGTGGA	CTTAACGCTCTCCTCGGTGT	IDT, Coralville
Pkm2	GTCTGAATGAAGGCAGTCCC	GTCCGCTCTAGGTATCGCAG	IDT, Coralville
LdhA	TGTCTCCAGCAAAGACTACTGT	GACTGTACTTGACAATGTTGGGA	IDT, Coralville
MCT4	TCACGGGTTTCTCCTACGC	GCCAAAGCGGTTCACACAC	IDT, Coralville
Slc1a5	GGACGT CTT CTATCTCCACAA	ACTCCTTCA ATGATGCCA CC	IDT, Coralville
Slc3a2	TGCAACCAAGAACTCAGA GC	TCATTTTGGACCTCACTCCC	IDT, Coralville
Slc7a5	ACAGCTGTGAGGAGCAGCAC	TCTTCGCCACCTACTTGCTC	IDT, Coralville
Gfpt1	GCCAACGCCTGCAAAATCC	GCCCAACGGGTATGAGCTAT	IDT, Coralville
Gfpt2	TGATGGGAATAACCACGAAGTCA	CGAAGTGTGTCTCAAACTCCAC	IDT, Coralville
Ppat	GGGAGTGCAGTGCCTAAATTC	GTACCTCGTATGTCCGATTCCA	IDT, Coralville
Gls	GCTGTGCTCTATTGAAGTGACA	TTGGGCAGAAACCACCATTAG	IDT, Coralville
Gls2	TGCATATAGTGGAGATGTCTCG	GCTCCATATCCATGGCCGACAA	IDT, Coralville
Glud1	CCCAACTTCTTCAAGATGGTGG	AGAGGCTCAACACATGGTTGC	IDT, Coralville
Got1	ACCGCACAGATGAATCTCAGC	ATGGGCAGGTACTCGTGGT	IDT, Coralville
Got2	TGGGCGAGAACAATGAAGTGT	CCCAGGATGGTTTGGGCAG	IDT, Coralville
Oat	TGCCACCCAAAGATCATAGATGC	TGTACTCCTCGTATTCACCAAGG	IDT, Coralville
Klf2	CTCAGCGAGCCTATCTTGCC	CACGTTGTTTAGGTCCTCATCC	IDT, Coralville
CCR7	GTCTCTCTCCAGCTAGCCCA	CAAACAGGAGCTGATGTCCA	IDT, Coralville
Cpt1a	TCTATGAGGGCTCGCG	CGTCAGGGTTGTAGCA	IDT, Coralville

PGC1α	TGAGGACCGCTAGCAAGTTT	TGTAGCGACCAATCGGAAAT	IDT, Coralville
Csf2	GGCCTTGGAAGCATGTAGAGG	GGAGAACTCGTTAGAGACGACTT	IDT, Coralville
IL23r	TTCAGATGGGCATGAATGTTTCT	CCAAATCCGAGCTGTTGTTCTAT	IDT, Coralville
IL22	ATGAGTTTTTCCCTTATGGGGAC	GCTGGAAGTTGGACACCTCAA	IDT, Coralville
GzmB	GCCCACAACATCAAAGAACAG	AACCAGCCACATAGCACACAT	IDT, Coralville
Tbx21	AGCAAGGACGGCGAATGTT	GGGTGGACATATAAGCGGTTC	IDT, Coralville
Tcf7	GTGGACTGCTGAAATGTTCG	AGCATCCGCAGCCTCAAC	IDT, Coralville
Bcl6	GATACAGCTGTCAGCCGGG	AGTTTCTAGGAAAGGCCGGA	IDT, Coralville
β-catenin	ATGGAGCCGGACAGAAAAGC	CTTGCCACTCAGGGAAGGA	IDT, Coralville
β–actin	ACGTAGCCATCCAGGCTGGTG	TGGCGTGAGGGAGAGCAT	IDT, Coralville
Human qPCR primer: 5'-3'			
Tcf7	AGAGAGAGAGTTGGGGGACA	TCTGCTCATGCATTACCCAC	IDT, Coralville
Bcl6	CTGGCTTTTGTGACGGAAAT	GTTTCCGGCACCTTCAGACT	IDT, Coralville
Lef1	CACTGTAAGTGATGAGGGGG	TGGATCTCTTTCTCCACCCA	IDT, Coralville
CD62L	CTTTCACCAAGGGCGATTTA	GGCATTTATCATTTGGCTGG	IDT, Coralville
Hprt1	TTTGCTTTCCTTGGTCAGGC	GCTTGCGACCTTGACCATCT	IDT, Coralville